

Nonlinear Instability of kink oscillations due to shear motions

J. Terradas, J. Andries¹, M. Goossens

jaume@wis.kuleuven.be

*Centre for Plasma Astrophysics and Leuven Mathematical Modeling and Computational
Science Centre*

Katholieke Universiteit Leuven, Celestijnenlaan 200B, B-3001 Leuven, Belgium

and

I. Arregui, R. Oliver, J. L. Ballester

Departament de Física, Universitat de les Illes Balears, E-07122 Palma de Mallorca, Spain

ABSTRACT

First results from a high-resolution three-dimensional nonlinear numerical study of the kink oscillation are presented. We show in detail the development of a shear instability in an untwisted line-tied magnetic flux tube. The instability produces significant deformations of the tube boundary. An extended transition layer may naturally evolve as a result of the shear instability at a sharp transition between the flux tube and the external medium. We also discuss the possible effects of the instability on the process of resonant absorption when an inhomogeneous layer is included in the model. One of the implications of these results is that the azimuthal component of the magnetic field of a stable flux tube in the solar corona, needed to prevent the shear instability, is probably constrained to be in a very specific range.

Subject headings: MHD — Sun: corona — Sun: magnetic fields — waves

1. Introduction

Coronal loops and filament threads are magnetic flux tubes whose field lines are anchored to the dense photosphere. Usually these structures are modeled as circular tubes whose

¹Postdoctoral Fellow of the National Fund for Scientific Research–Flanders (Belgium) (F.W.O.-Vlaanderen).

properties change mainly in the radial direction with a sharp or a smooth transition. Using the ideal magnetohydrodynamic (MHD) equations the eigenmodes of cylindrical magnetic tubes can be calculated. A fundamental eigenmode of oscillation is the kink mode, with an azimuthal number $m = 1$, which produces a transverse displacement of the tube. Examples of the calculations of the kink mode for sharp interfaces can be found in Spruit (1981); Edwin & Roberts (1983); Cally (1986) and for smooth transition layers in Goossens et al. (1992); Ruderman & Roberts (2002); Van Doorselaere et al. (2004); Terradas et al. (2006). In the last case, the coupling of compressional fast magnetohydrodynamic (MHD) waves and shear Alfvén waves leads to the formation of resonances in the inhomogeneous layers and this mechanism is a possible candidate to explain the damping of transverse coronal loop oscillations (Hollweg & Yang 1988; Ruderman & Roberts 2002; Goossens et al. 2002) and filament threads (Arregui et al. 2008).

So far, most of the theoretical studies about the kink mode are in the linear regime and second order perturbations are neglected in the MHD equations, however, there are some observational indications suggesting that this assumption might be not fully justified in all the oscillating loops (Terradas & Ofman 2004). Nonlinearity adds new and interesting effects. For example, the ponderomotive force creates a flow along the field lines (Rankin et al. 1994; Tikhonchuk et al. 1995), and for the standing kink oscillation it tends to accumulate mass at the loop apex (Terradas & Ofman 2004). When gas pressure is taken into account, the otherwise unlimited accumulation of mass is prevented by the pressure forces which limit the secular growth and produce saturation in the density.

Another possible consequence of the nonlinearity is the generation of instabilities. It is well known that even in the linear regime, a sharp interface between two media in relative motion is liable to the Kelvin-Helmholtz instability (KHI). In the presence of a magnetic field, KHI of a flow parallel to the field lines in a homogeneous medium sets in if the velocity jump exceeds the maximum Alfvén speed. The criteria for the KHI for an axial flow is modified in the presence of a boundary layer of finite width, which also induces the possibility of resonant flow instabilities (see Hollweg et al. 1990; Yang & Hollweg 1991; Andries & Goossens 2001a,b). The effect of an azimuthal flow is less explored in the literature. Heyvaerts & Priest (1983); Browning & Priest (1984) showed that azimuthal shear motions in the presence of a smooth transition layer can be KH unstable. The most likely place for the KHI to occur is where the velocity is largest and the magnetic field is perpendicular to the velocity (see for example Rankin et al. 1993). For the fundamental standing kink mode this is precisely the antinode of the velocity, located at half the loop length from the photosphere.

In this Letter we report on the nonlinear evolution of the kink oscillation of a tube with-

out twist. The full nonlinear three-dimensional ideal MHD equations are solved numerically. From the simulations we investigate the motions in the magnetic tube and show the first results of the development of the nonlinear shear instability at the tube boundary.

2. Tube Model and Initial Conditions

The system under consideration is a compressible plasma that obeys the general equations of MHD. The equilibrium magnetic field is straight, uniform, and pointing in the z -direction. In a cylindrical coordinate system with the axis along the magnetic field, the density of the circular tube changes with the radial coordinate from ρ_{in} inside the tube to ρ_{ex} in the coronal medium through an inhomogeneous layer of width l . The length of the loop is L and the mean radius R . To have magneto-hydrostatic equilibrium the gas pressure is uniform, and the plasma- β is chosen to be small, 5×10^{-2} (we assume a sound speed of $c_s = 0.2 v_{\text{Ai}}$, where v_{Ai} is the Alfvén velocity inside the tube). In this model the role played by the non-zero gas pressure is important since it avoids the continuous accumulation of mass at the tube half length due to the nonlinear ponderomotive force. We apply line-tying conditions at the planes located at $z = 0$ and $z = L$ to mimic the anchoring in the photosphere and to obtain a standing mode.

The system is perturbed with the spatial structure of the linear fundamental standing kink eigenmode ($m = 1$, and longitudinal wavenumber $k_z = \pi/L$) of a magnetic tube with a discontinuous density profile. This allows exciting a single eigenmode (in the linear regime) and avoiding a significant excitation of leaky modes. For this disturbance the radial component of the velocity is continuous across the loop boundary while the azimuthal component has a jump at the boundary. The initial perturbation is the seed of the instability in the nonlinear regime. The amplitude of the initial velocity perturbation at the center of the tube ($x = 0, y = 0$) is v_0 . Another relevant magnitude in our analysis is the axial component of the vorticity, $\Omega_z = (\nabla \times \mathbf{v}) \cdot \hat{\mathbf{e}}_z$. The initial kink perturbation is a vortex sheet at the tube boundary (see Fig. 1a).

The radial, azimuthal, and longitudinal dependence of the initial perturbation are transformed to the 3D Cartesian system of our computational box. Given the initial condition the time-dependent nonlinear MHD equations are numerically solved. We have used an explicit high-order numerical scheme (*4th*-order in time and *3th*-order in space) based on the method of lines to solve the equations in conservative form (see Terradas et al. 2008, for further details). Due to the resolution requirements the parallelized version of the code has been run in a cluster of machines. We have used a grid resolution of $512 \times 512 \times 100$ points since the small scales are in the $x - y$ plane while the solution is smooth in the z -direction.

3. Tube Evolution

We have started the analysis of the evolution of the tube with very small amplitudes of the initial perturbation ($v_0 \ll v_{Ai}$). From the fully 3D problem we recover the linear results, i.e. the loop oscillates around the equilibrium position as a whole with the kink mode frequency. If instead of a sharp density transition between the tube and the external medium we use a smooth density profile (we have used thick layers to have enough grids points inside the resonant layer), then the tube attenuates due to the energy conversion between the fast MHD waves and the Alfvén waves in the layer. We have found that the period and damping time are in good agreement with the theoretical linear predictions.

The behavior of the system changes completely when we are in the nonlinear regime. The first effect is the generation of flows along the tube axis produced by the nonlinear terms. However, these flows are much smaller (in the regime considered here) than the local Alfvén speed and therefore unable to generate an instability. The dynamics of the system is dominated by the azimuthal flows at the tube boundary.

3.1. Sharp transition layer

We first consider a sharp transition between the tube and the external medium. The evolution of the density and the longitudinal component of the vorticity of a representative case in a weak nonlinear regime is shown in Figure 1 at different time intervals. To visualize the results of the 3D simulations we concentrate on the plane at half the tube length where we expect the strongest nonlinear effects. The initial perturbation produces a lateral displacement of the tube in the x -direction. As in the linear regime the tube starts to oscillate around the initial position, but small length scales quickly develop at the boundary. We can appreciate this, for example, around the points $x = 0$ and $y = \pm R$ (see Fig. 1b), which is the position where v_x has a maximum jump. These small scale structures grow with time (see Fig. 1c) and several rolls form at the loop boundary. Note that around $x = \pm R$ and $y = 0$ the density is almost undisturbed because there are no shear motions at this position. At later stages of the evolution (Fig. 1d) the small spatial scales are still localized at the boundary and eventually the system reaches a saturation state. As a result of the instability the overall shape of the tube at the boundary has been considerably altered and a rather inhomogeneous layer has been generated. The changes at the tube boundary are also clear in the vorticity. In the early phase the initial vortex sheet, located at the boundary, shows small and localized deformations (Fig. 1b). Since the tube is oscillating the flow changes sign in each oscillation, and the vortex sheet evolves in a complex way, showing a very undulated shape (Figs. 1c and 1d).

3.2. Smooth transition layer

Now we assume that the equilibrium already has a transition region. The main difference with respect to the previous case is that the resonant absorption process induces shear motions at the inhomogeneous layer due to phase mixing. The results are represented in Figure 2 for two different widths of the layer at a given time instant (same as in Fig. 1c). We see that the instability is also present (Fig. 2a), but now it is less developed in comparison with the sharp transition case (Fig. 1c). We also see (Fig. 2b) that the thicker the layer the slower the growth-rate of the instability (in Fig. 2b the instability is still not present). Since the boundary of the tube eventually changes its shape due to the instability, a question that arises is how this affects the process of resonant absorption. We have calculated the damping rate (damping time over period) of the tube from the simulations for the two cases considered in Figure 2 (calculating the displacement of the central point of the tube). The numerical estimates give values around 1.9 for $l = 0.5R$ and 1.2 for $l = R$, while the linear values of the damping rates based on eigenmode calculations are 2.4 and 1.1, respectively. The differences are small, indicating that the instability, for the particular parameters considered here, does not change much the efficiency of the energy conversion.

4. Discussion and Conclusions

The numerical results shown in this Letter indicate that the shear motions involved in the kink oscillations of a magnetic tube might be unstable. The instabilities are found to create small length scales in the azimuthal direction and grow rapidly in time. For a cylindrical discontinuous interface between two homogeneous stationary rotating fluids the following growth rates (imaginary part of the frequency) of the Kelvin Helmholtz instability can be readily derived:

$$\omega_i^2 = \frac{\rho_{\text{in}}\rho_{\text{ex}}}{(\rho_{\text{in}} + \rho_{\text{ex}})^2} \frac{m^2}{R^2} 4v_0^2 - 2k_z^2 \frac{B_0^2}{\mu(\rho_{\text{in}} + \rho_{\text{ex}})}. \quad (1)$$

Here $2v_0$ is the amplitude of the velocity shear at the boundary. The derivation involves the assumption that the azimuthal length scales are much smaller than the longitudinal ones (which is the case for the instabilities that formed in our study). Clearly the background equilibrium for which equation (1) is obtained is very different from the shear motions associated to the kink mode oscillations, which depend on time, ϕ and z . Nevertheless, the small scales and the localization of the instabilities in the azimuthal direction, and the fast growth rates, suggest that equation (1) may be considered as a local analysis and we need not to worry about the azimuthal and time dependence of the shear motions. For the parameters considered in §3, the first unstable mode corresponds to $m = 5$ (which satisfies the

assumption of azimuthal localization), and its growth rate is $1/\omega_i \approx 5.0\tau_A$. The important point here is that it is smaller than the kink period, around $16.3\tau_A$ (satisfying the assumption of localization in time). Moreover, this calculation also clarifies that the most unstable modes will have small azimuthal length scales but large longitudinal length scales, since this minimizes the stabilizing force induced by the bending of the field lines. However, the large longitudinal length scales prevent to interpret equation (1) as a local approximation in z since the velocity shear is less than $2v_0$ throughout most of the loop. Growth rates are thus expected to be somewhat smaller, and instability will set in only for azimuthal length scales smaller than those predicted by equation (1). An appropriate analysis thus needs to take into account the longitudinal variation of the shear profile and hence necessarily involves a 2D model.

We have found that the evolution of the tube is very sensitive to the amplitude of the initial perturbation. As expected, the larger the amplitude of the initial perturbation the faster the development of the instability. By changing the initial amplitude of the perturbation in a broad range, an extended transition layer (even much larger than the developed in Fig. 1) may naturally evolve as the result of the shear instability of a sharp transition between the flux tube and the external medium. In addition, for very large amplitudes the tube might show severe deformations, a wake can even form behind the tube and it can interact with the main body in each oscillation, the final shape of the tube being rather irregular.

When an inhomogeneous layer between the tube and the environment is included then the motions are characterized by phase-mixed scales and the instability is also present. Nevertheless, the instability develops more slowly than in the sharp transition case. This is probably due to the fact that the thicker the layer the later the generation of small length scales due to the phase mixing process, and thus the onset of the instability. This situation seems to be related to the development of the KHI for torsional Alfvén waves ($m = 0$) described by Browning & Priest (1984) (see also Walker 1981). Interestingly, for the regime studied here (basically thick layers) the attenuation of the central part of the tube due to resonant absorption is not significantly altered by the changes at the boundary due to the shear instability.

In the context of coronal loops an immediate question that arises from the results presented here is why, up to now, there is no clear evidence of such instability from the observation of oscillating loops. There are several partial answers. Magnetic twist, not included in our model, might decrease or even suppress the instability since the presence of a magnetic field component along the flow stabilizes the KHI. Several examples of the stabilizing effect of a helical magnetic field component can be found in rising tubes in the convection zone (see

for example Moreno-Insertis & Emonet 1996) or in stellar jets. On the other hand, a tube with very large azimuthal magnetic field is subject to the instabilities of the linear pinch (typically for a twist larger than 2.5π , although it depends on the details of the equilibrium and boundary conditions). Therefore, the azimuthal component of the magnetic field of a stable flux tube in the solar corona is probably constrained to be in a specific range (being 2.5π an upper bound for the twist). Other factors that could explain the absence of observational evidences of the instability are that it is not spatially resolved with the current spatial resolution of the telescopes or simply that the amplitude of the oscillating loops is not strong enough to develop the instability. However, the tube displacement produced by the initial perturbation in our simulations is of the order of and even smaller than the observed amplitudes of oscillation in loops, so this last possibility seems to be ruled out.

We have given a qualitative description of the shear instability, but a quantitative analysis (with improved numerical resolution) about the growth rates of the modes, and a detailed study of the effect of the instability on the damping rates under different regimes is still needed. In addition, the equilibrium configuration should be improved in several aspects. For example, a more accurate model should incorporate a realistic variation of the density and temperature from the photosphere to the corona. However, the inclusion of a twisted magnetic field for the reasons mentioned before seems to be the most relevant aspect that needs to be addressed.

J. Terradas is grateful to the Research Council fellowship F/06/65 of the KUL. Spanish funding provided under grants AYA2006-07637 and PCTIB-2005GC3-03 is acknowledged. We are grateful to Fernando Moreno-Insertis for his comments and suggestions.

REFERENCES

- Andries, J., & Goossens, M. 2001a, *A&A*, 368, 1083
- Andries, J., & Goossens, M. 2001b, *A&A*, 375, 1100
- Arregui, I., Terradas, J., Oliver, R., & Ballester, J. L. 2008, *ApJ*, 682, L141
- Browning, P. K., & Priest, E. R. 1984, *A&A*, 131, 283
- Cally, P. S. 1986, *Sol. Phys.*, 103, 277
- Edwin, P. M., & Roberts, B. 1983, *Sol. Phys.*, 88, 179,
- Goossens, M., Hollweg, J. V., & Sakurai, T. 1992, *A&A*, 138, 233

- Goossens, M., Andries, J., & Aschwanden, M. J. 2002, *A&A*, 394, L39
- Heyvaerts, J., & Priest, E. R. 1983, *A&A*, 117, 220
- Hollweg, J. V., & Yang, G. 1988, *J. Geophys. Res.*, 93, A6, 5423
- Hollweg, J.V., Yang, G., Cadez, V.M., & Gakovic, B. 1990, *ApJ*, 349, 335
- Moreno-Insertis, F., & Emonet, T. 1996, *ApJ*, 472, L53
- Rankin, R., Harrold, B. G., Samson, J. C., & Frycz, P. 1993, *J. Geophys. Res.*, 98, A4, 5839
- Rankin, R., Frycz, P., Tikhonchuk, V. T., & Samson, J. C. 1994, *J. Geophys. Res.*, 99, 21291
- Ruderman, M. S., & Roberts, B. 2002, *ApJ*, 577, 129
- Spruit, H. C. 1982, *Sol. Phys.*, 75, 3
- Terradas, J., & Ofman, L. 2004, *ApJ*, 610, 523
- Terradas, J., Oliver, R., & Ballester, J. L. 2006, *ApJ*, 642, 533
- Terradas, J., Oliver, R., & Ballester, J. L., Keppens, R. 2008, *ApJ*, 675, 875
- Tikhonchuk, V. T., Rankin, R., Frycz, P., & Samson, J. C. 1995, *Phys. Plasmas*, 2, 501
- Van Doorselaere, T., Andries, J., Poedts, S., & Goossens, M. 2004, *ApJ*, 606, 1223
- Walker, A. D. M. 1981, *Planet. Space. Sci*, 29, 10, 1119
- Yang, G., & Hollweg, J.V. 1991, *J. Geophys. Res.*, 96, 13807

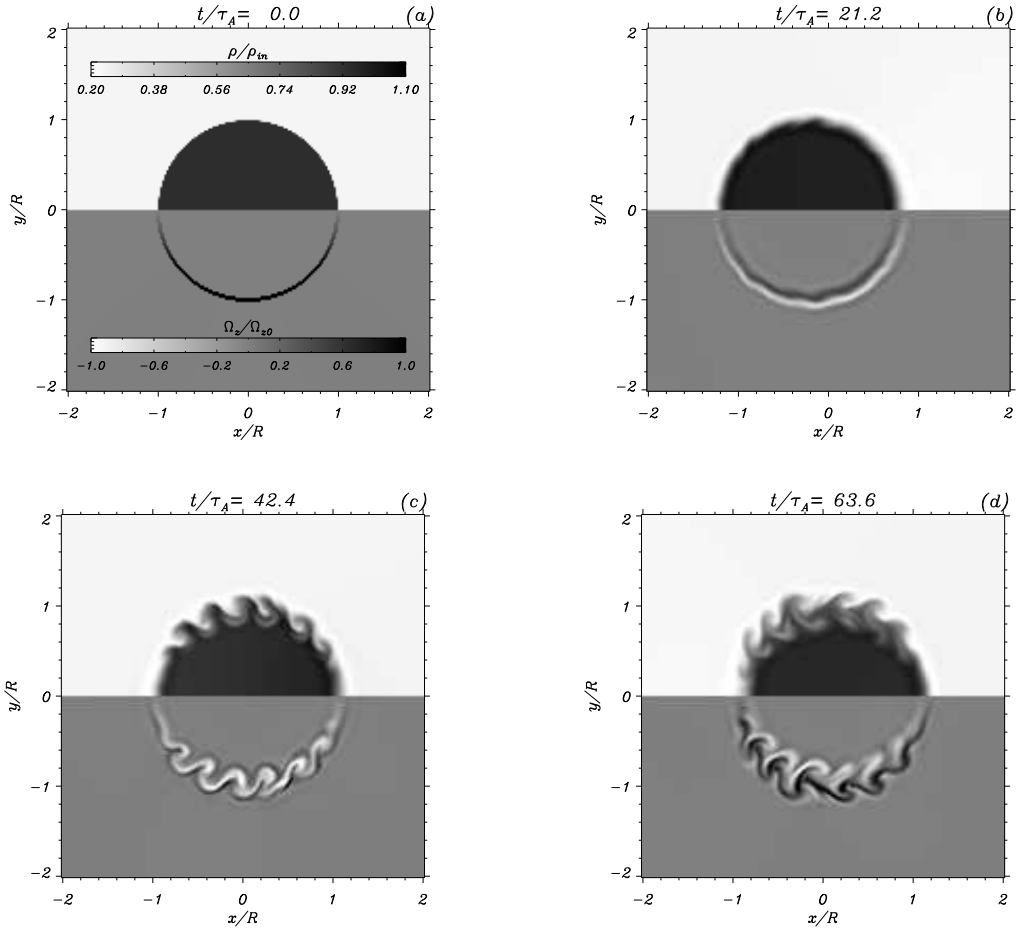


Fig. 1.— The top half of each panel displays the density (symmetric respect to $y = 0$) and the bottom half the vorticity (antisymmetric respect to $y = 0$) at $z = L/2$ for different times. In this simulation the following parameters have been used: $L = 10R$, $\rho_{\text{in}}/\rho_{\text{ex}}=3$, $v_0 = 0.1v_{\text{Ai}}$, and a full domain of $[-6R, -6R] \times [-6R, 6R] \times [0, 10R]$. Lengths are normalized to the loop radius, R (typically of the order of 4000 km), velocities to the internal Alfvén velocity, $v_{\text{Ai}} = B_0/\sqrt{\mu\rho_{\text{in}}}$ (of the order of 1000 kms^{-1}), and time to the Alfvén crossing time, $\tau_A = R/v_{\text{Ai}}$. *This figure is available as an mpeg animation in the electronic edition of the Journal.*

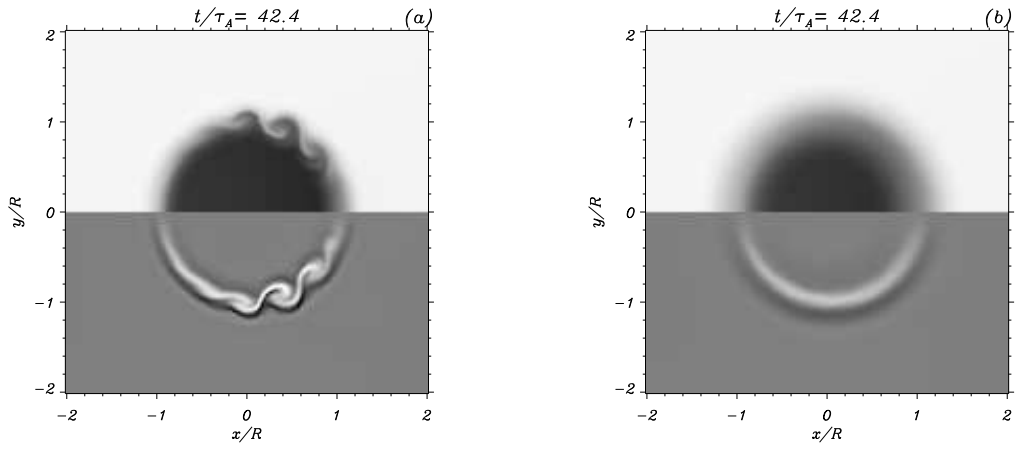


Fig. 2.— Density and vorticity (for the same time instant as in Fig. 1c) for two different widths of the inhomogeneous layer connecting the tube and the external medium, **a)** $l = 0.5R$ and **b)** $l = R$. All other parameters are the same as in Figure 1.